Naval Research Laboratory
Washington, DC 20375-5320

NRL/MR/6750--06-8992

Hollow Cathode Produced Electron Beams for Plasma Generation: Cathode Operation in Gas Mixtures

Scott Walton
Darrin Leonhardt
Richard Fernsler

Charged Particle Physics Branch
Plasma Physics Division

December 15, 2006

Approved for public release; distribution is unlimited.

REPORT DOCUMENTATION PAGE

Form Approved
OMB No. 0704-0188

Public reporting burden for this collection of information is estimated to average 1 hour per response, including the time for reviewing instructions, searching existing data sources, gathering and maintaining the data needed, and completing and reviewing this collection of information. Send comments regarding this burden estimate or any other aspect of this collection of information, including suggestions for reducing this burden to Department of Defense, Washington Headquarters Services, Directorate for Information Operations and Reports (0704-0188), 1215 Jefferson Davis Highway, Suite 1204, Arlington, VA 22202-4302. Respondents should be aware that notwithstanding any other provision of law, no person shall be subject to any penalty for failing to comply with a collection of information if it does not display a currently valid OMB control number. **PLEASE DO NOT RETURN YOUR FORM TO THE ABOVE ADDRESS.**

1. REPORT DATE *(DD-MM-YYYY)*	2. REPORT TYPE	3. DATES COVERED *(From - To)*
15-12-2006	Memorandum Report	

4. TITLE AND SUBTITLE

Hollow Cathode Produced Electron Beams for Plasma Generation: Cathode Operation in Gas Mixtures

5a. CONTRACT NUMBER

5b. GRANT NUMBER

5c. PROGRAM ELEMENT NUMBER

6. AUTHOR(S)

Scott Walton, Darrin Leonhardt, and Richard Fernsler

5d. PROJECT NUMBER
67-7641-07

5e. TASK NUMBER

5f. WORK UNIT NUMBER

7. PERFORMING ORGANIZATION NAME(S) AND ADDRESS(ES)

Naval Research Laboratory
4555 Overlook Avenue, SW
Washington, DC 20375-5320

8. PERFORMING ORGANIZATION REPORT NUMBER

NRL/MR/6750--06-8992

9. SPONSORING / MONITORING AGENCY NAME(S) AND ADDRESS(ES)

Office of Naval Research
One Liberty Center
875 North Randolph Street
Arlington, VA 22203-1995

10. SPONSOR / MONITOR'S ACRONYM(S)

11. SPONSOR / MONITOR'S REPORT NUMBER(S)

12. DISTRIBUTION / AVAILABILITY STATEMENT

Approved for public release; distribution is unlimited.

13. SUPPLEMENTARY NOTES

14. ABSTRACT

Pulsed hollow cathode discharges, used to generate kilovolt electron beams for the production of plasmas, were studied in low pressure (50-70 mTorr) backgrounds of argon, oxygen, nitrogen, SF_6 and mixtures thereof. Cathode currents were measured as a function of cathode voltage, duty factor, and relative gas concentration. The cathode current was found to have a dependence on all variables, with the greatest impact being operating gas for all voltages and duty factors. The ambient gas is thought to influence the production of secondary electrons at the cathode surface, thereby impacting the operation of the hollow cathode discharge and electron beam production.

15. SUBJECT TERMS

Plasma production and diagnostics
Hollow cathode
Secondary electron emission

16. SECURITY CLASSIFICATION OF:			17. LIMITATION OF ABSTRACT	18. NUMBER OF PAGES	19a. NAME OF RESPONSIBLE PERSON
a. REPORT	b. ABSTRACT	c. THIS PAGE			Scott Walton
Unclassified	Unclassified	Unclassified	UL	20	19b. TELEPHONE NUMBER *(Include area code)* (202) 767-7531

Standard Form 298 (Rev. 8-98)
Prescribed by ANSI Std. Z39.18

Hollow Cathode Produced Electron Beams for Plasma Generation: Cathode Operation in Gas Mixtures

Scott G. Walton, Darrin Leonhardt, and Richard F. Fernsler
Plasma Physics Division, US Naval Research Laboratory, Washington, DC 20375

Abstract

Pulsed hollow cathode discharges, used to generate kilovolt electron beams for the production of plasmas, were studied in low pressure (50-70 mTorr) backgrounds of argon, oxygen, nitrogen, SF_6 and mixtures thereof. Cathode currents were measured as a function of cathode voltage, duty factor, and relative gas concentration. The cathode current was found to have a dependence on all variables, with the greatest impact being operating gas for all voltages and duty factors. The ambient gas is thought to influence the production of secondary electrons at the cathode surface, thereby impacting the operation of the hollow cathode discharge and electron beam production.

I. INTRODUCTION

A. Background

An electron beam generated plasma is the foundation of the Naval Research Laboratory's Large Area Plasma Processing System (LAPPS), which has been utilized in a number of materials processing applications ranging from deposition to etching to surface activation. High-energy (1-5 keV) electron beams are an efficient way to ionize a gas and thus produce a high-density (10^{10} – 10^{12} cm^{-3}) plasma over the volume of the beam. Typically, LAPPS uses a sheet-like electron beam where the beam thickness is preserved by the presence of co-axial magnetic field, usually about 150 Gauss. Beam dimensions vary depending on the beam source geometry (width and thickness), beam energy and operating pressure (length) but, for multi-kilovolt beams in 50 – 500 mTorr operating pressures, the system is capable of processing surface areas on the order of a square meter.

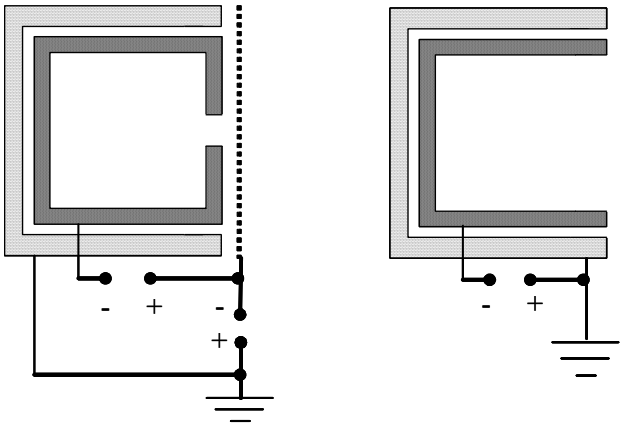

Fig. 1 Hollow cathode configurations. (Left) Closed face hollow cathode used at NRL for continuous e-beam production. (Right) Open face hollow cathode used in this work for pulsed, electron beam production.

For processing applications the electron beam source must be able to sustain multi-kilovolt beams with high current densities (10's mA/cm^2) over long periods of time, while operating in reactive gas backgrounds and/or pressures typically above 1 mTorr. For these requirements, a simple yet practical choice for an electron beam source is a cold cathode or glow discharge electron gun in the form of a hollow cathode. In these sources, plasma

production is enhanced by the 'hollow cathode effect', which describes electron reflection between the cathode walls, resulting in much larger beam currents. These hollow cathode sources can be characterized into two general types: "closed face" and "open face" (see Fig. 1). The difference between the two is not only geometry but also in how the electron beam is produced. For the closed face geometry, a small fraction of the plasma electrons become beam electrons after acceleration across the cathode sheath (or other such accelerating voltage) outside the hollow cathode aperture. In the open face guns, it is the secondary electrons emitted from the cathode walls that form the beam electrons [1]. The latter is the primary electron beam source used in LAPPS [2] and the focus of this paper.

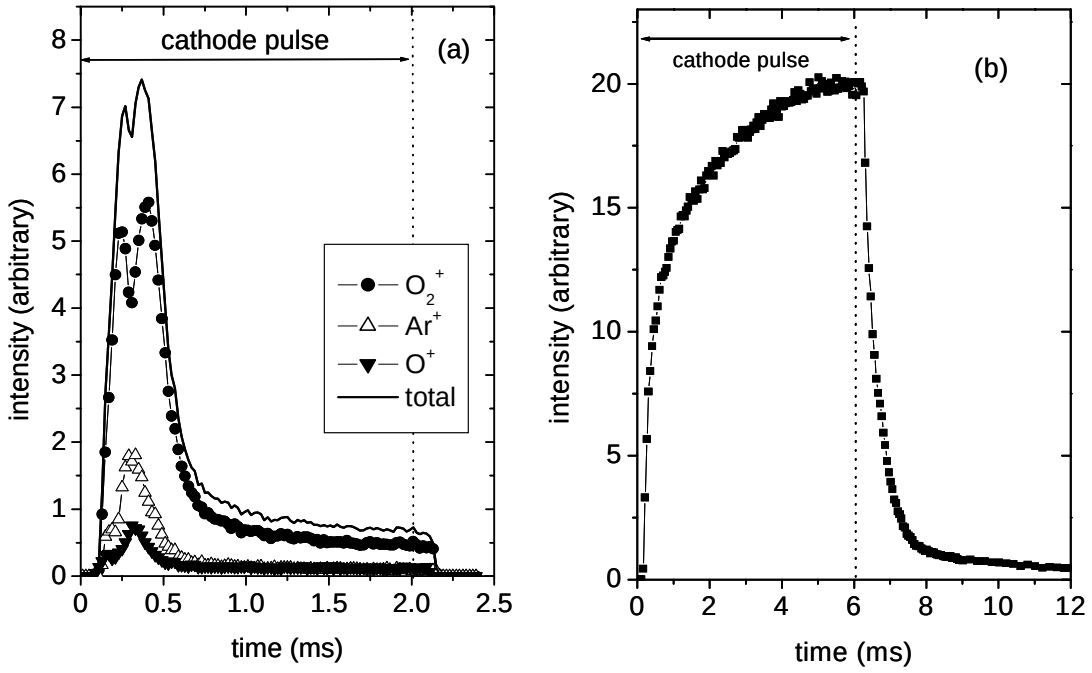

Fig. 2 (a) Ion flux measurements in 50:50 Argon-Oxygen mixtures (from Ref. 3). (b) Ion flux measurements in pure Argon (from Ref. 4).

B. Motivation

The experiments in this paper were undertaken to understand recent ion flux measurements shown in Fig. 2(a). The fluxes were measured at electrodes located adjacent to electron beam generated plasmas produced in 50:50 mixtures of argon and oxygen [3]. The results are characterized by a large peak in the total and mass-resolved ion fluxes shortly after plasma initiation and are in contrast to measurements shown in Fig. 2(b) for plasmas produced in pure argon [4], where the ion flux grows monotonically toward steady state. In these experiments, the ion flux is proportional to the plasma density, which evolves as

$$\frac{dn_i}{dt} = k_b j_b - \beta n_e n_i - \frac{D_a}{l^2} n_i . \qquad (1)$$

The first term on the right hand side is the source term described by the ionization rate (k_b) and the electron beam density (j_b). The other two terms on the right are the destruction terms,

where β is the electron-ion recombination rate, D_a is the ambipolar diffusion constant, l is the diffusion length, and n_e and n_i are the electron and ion densities, respectively. In pure argon (Fig. 2b), the behavior has been previously described in [4] and has been shown to depend mainly on the ambipolar diffusion of species. However, in mixtures containing large amounts of molecular gases, the diffusion term can be neglected for any significant diffusion length. Setting $n_e \approx n_i$, the solution for a constant beam current becomes,

$$n_i(t) = A\frac{\exp(A\beta t) - \exp(-A\beta t)}{\exp(A\beta t) + \exp(-A\beta t)}; A = \sqrt{\frac{k_b j_b}{\beta}}. \quad (2)$$

Thus, the measured ion flux shown in Fig. 2a can *not* be explained by gas phase reactions alone and likely requires a time dependent electron beam.

A comparison of the cathode currents measured for each background mixture using identical cathode pulses (2 kV, 10% duty) is shown in Fig. 3. The obvious differences are the

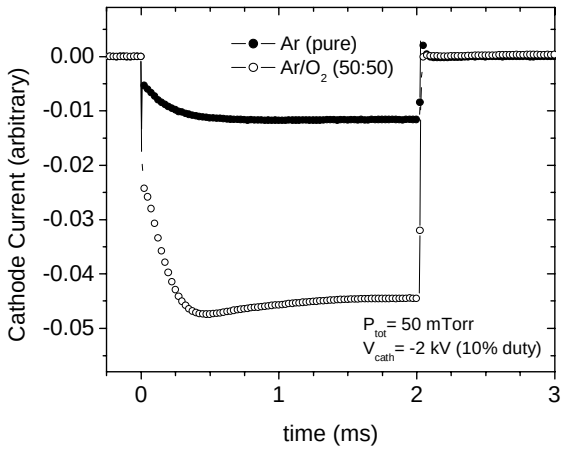

Fig. 3 Cathode current measurements corresponding to the results from Fig. 2. The total pressure was 50 mTorr and the cathode was modulated using a 2 kV pulse operating at a 10% duty factor.

magnitude and the temporal behavior of the currents. For argon, the current increases smoothly to a steady state value while for the oxygen-argon mixtures, the current reaches a maximum before attaining a steady state. This difference suggests that a correlation may exist between cathode operation, electron beam operation, and downstream plasma characteristics; a correlation that might explain the ion flux behavior observed in Fig. 2.

The present experiments were designed to address two broad questions. First, why is the cathode current, in oxygen mixtures different from pure argon? That is, what physical phenomenon leads to a larger cathode current and why is the temporal behavior altered with the addition of oxygen? Second, how is cathode operation related to plasma production and the measured ion fluxes? More specifically, are changes in cathode operation producing a strong temporal variation in electron beam production? It is worth noting that a better understanding of this behavior is more than cathode physics, since cathode operation is a critical component in the development of this materials processing system.

II. EXPERIMENTAL

Two chambers were used for these experiments, and both have been previously described. Most work was carried out in a rectangular, stainless steel chamber [4]. The Ar/SF_6 and one set of the Ar/O_2 experiments were performed in a cylindrical, aluminum chamber. Despite the chamber differences, internal system and cathode construction were similar and are represented in Fig. 4. The cathodes were encased in a grounded shield but separated from it by an insulator. Downstream is a grounded anode, which has a slot through which the emergent electron beam passes before terminating at a final ground anode. Because of system differences, a direct comparison of cathode current or ion flux magnitude is *not* useful, since differences in chamber geometries, cathode construction, and cathode-anode-anode lengths all influence plasma production. However, these nuances should not affect relative cathode operation in varying gas mixtures.

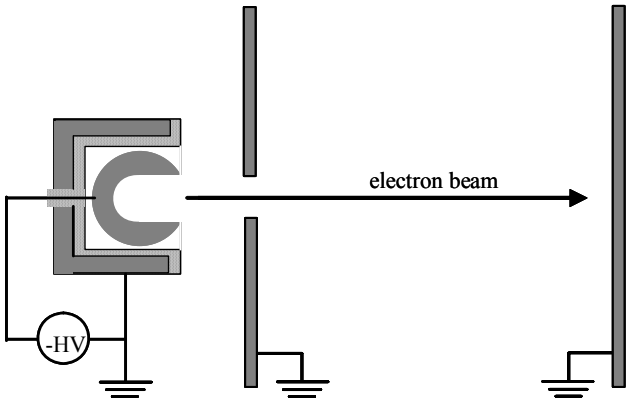

Fig. 4 General experimental setup used in this work consisting of a hollow cathode, a grounded anode with a slot through which the beam passes, and a grounded termination anode.

Gases were introduced via mass flow controllers and operating pressure was achieved by choking gas flow at the entrance to the turbo pumps using a gate valve. The gate valve was positioned to maintain the total pressure of pure argon at 50 sccm flow. For the gas mixtures, partial pressures were achieved by adjusting *relative* gas flows, and the molecular gas partial pressures were measured separately (i.e., in the absence of argon). Using this approach, the *total* gas flow and pressure were nominally constant. However, a small error (+/- 5%) is expected in the pressures given that the relative pumping speed of each gas is expected to vary in gas mixtures.

The cathode voltage was measured near the chamber feedthrough using a voltage divider, and the cathode current was measured using a Rogowski coil. The signals from each was fed to a digital oscilloscope and averaged over 1000 pulses. Before recording the signals, a few minutes were allowed to elapse to let the system settle into constant operation.

Ion currents at the stage were measured using a – 10V dc bias to repel plasma electrons. The current was determined by measuring the voltage drop across a 10 Ω resistor between the power supply and ground.

III. RESULTS

Cathode operation was first investigated under normal LAPPS operation with a 150 Gauss magnetic field. Shown in Fig. 5 are the cathode currents and stage currents measured simultaneously using variable oxygen flows. The cathode was pulsed to 2 kV for 3 ms at a 10% duty, and the total pressure was fixed at 50 mTorr. The current was found to increase with increasing oxygen concentration. At higher oxygen concentrations the current shows a slight peak before reaching steady state. The stage currents show a similar peak early in time,

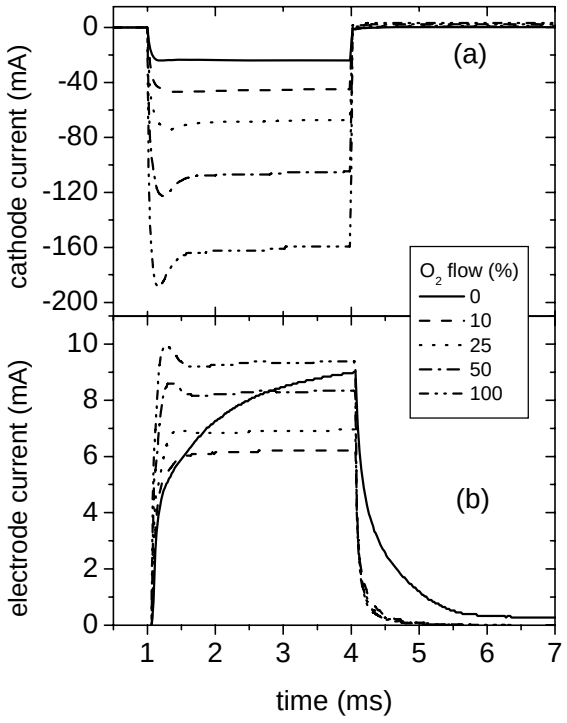

Fig. 5 (a) Cathode currents produced in various relative concentrations of O_2 in argon. (b) Ion currents measured at an electrode located between the two anodes in Fig. 4 and approximately 1.2 cm from the electron beam axis. A biased of -10 V_{dc} was applied to the electrode. Conditions were 100 sccm total gas flow, 50 mTorr total pressure, 2 kV cathode pulse, 3 ms pulse width, and a 10% duty.

and the results support the previous ion flux measurements [Fig 2(a)]. It is important to note that a direct comparison is difficult because the ion flux measurements of Fig. 2(a) were acquired at a grounded stage.

Shown in Fig. 6 is the temporal evolution of the cathode current in argon/oxygen as

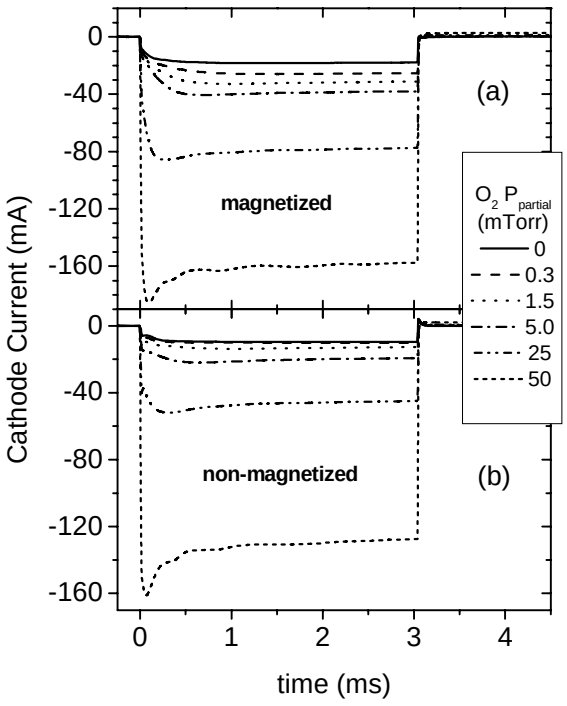

Fig. 6 Cathode current in various relative concentrations of O_2 in argon (a) with and (b) without the applied magnetic field. Conditions were 50 mTorr total pressure, 2 kV cathode pulse, 3 ms pulse width, and a 10% duty.

well as pure gases. The presence of the magnetic field will influence cathode operation, so the experiments were repeated in the absence of the magnetic field. As expected, the current increased with magnetic field strength, and especially so when the oxygen concentration was

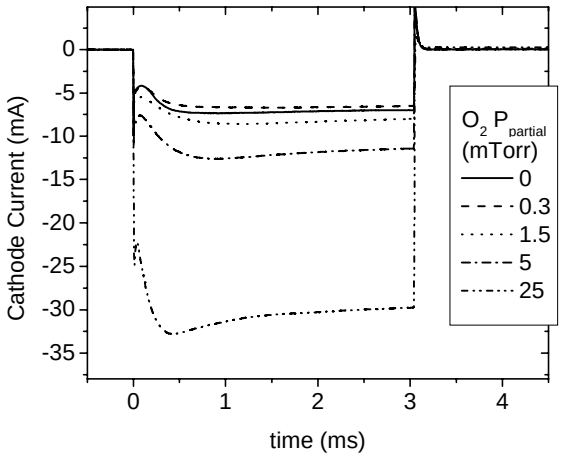

Fig. 7 Cathode current in various relative concentrations of O_2 in argon (50 mTorr total pressure) without the applied magnetic field and operating at a 30% duty factor.

less than 50%. The experiments in Ar/O_2 mixtures were repeated using higher duty factor cathode operation, again in the absence of the magnetic field. The results are shown in Fig. 7 for a cathode pulsed to 2 kV for 3 ms at a 30% duty. While the cathode current still increases with increasing oxygen concentration, the increase is smaller than for 10% duty factor operation.

Shown in Fig. 8 is the temporal evolution of the cathode current at various applied cathode voltages (10% duty). The total pressure was increased to 70 mTorr in these measurements to so that a reasonable cathode current could be achieved at the lowest

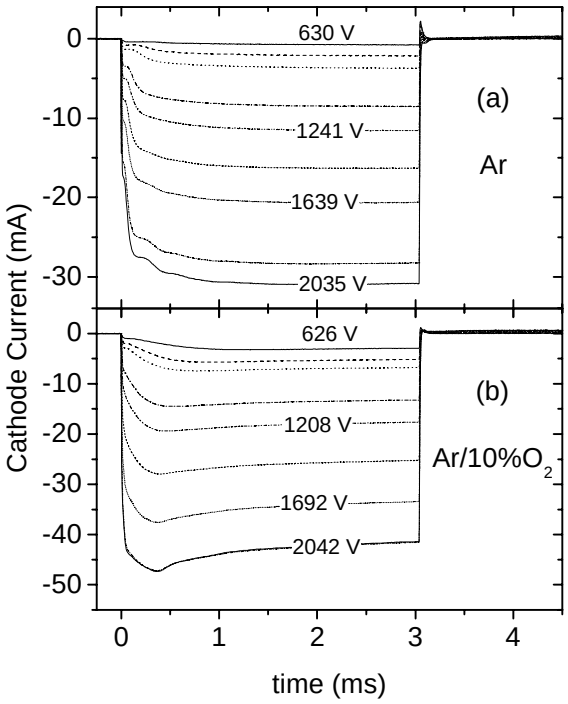

Fig. 8 Cathode current in (a) pure argon and (b) 10% O_2 in argon for a range of applied voltage pulses. Conditions were 70 mTorr total pressure, 3 ms pulse width, and a 10% duty.

applied cathode voltage. Fig. 8(a) shows the results in pure argon and Fig. 8(b) shows the results for Ar/O_2 mixtures containing approximately 10% oxygen.

In order to further determine the importance of oxygen in cathode operation, the experiments using a 2kV cathode pulse operating at 10% duty were repeated using nitrogen and SF_6 as diluting gases. Shown in Fig. 9 are the results for magnetized and non-magnetized cathode operation in Ar/N_2 mixtures and pure gases. In contrast to oxygen, increasing nitrogen serves to decrease the cathode current and only in the absence of a magnetic field does the cathode current show a maximum early in time at large nitrogen concentrations (ignoring any ignition effects). Experiments using SF_6 mixtures were performed in the aluminum chamber in the absence of a magnetic field. The results are shown in Fig. 10 and are very similar to those for oxygen; in particular, the magnitude increases with increasing SF_6 flow (with the exception of the lowest concentration), and the current has a maximum early in time at large concentrations.

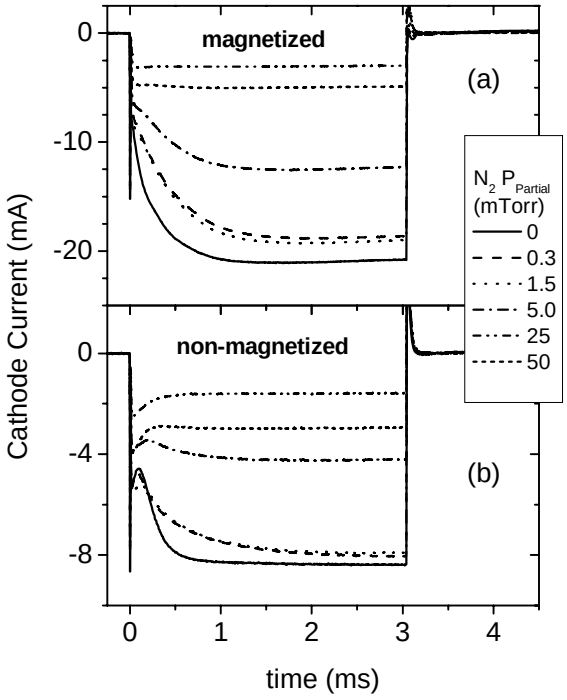

Fig. 9 Cathode current in various relative concentrations of N_2 in argon (a) with and (b) without the applied magnetic field. Conditions were 50 mTorr total pressure, 2 kV cathode pulse, 3 ms pulse width, and a 10% duty.

The results for all measurements are summarized in Fig. 11 where the average currents, over a selected range of times (see figure), are plotted as a function of partial gas pressure. The figure illustrates the increase or decrease in cathode current with increasing oxygen, SF_6, and nitrogen relative concentrations. For O_2, the increase in cathode current is less when the cathode voltage is modulated at a greater duty factor and a comparison of the normalized relative increases is shown in Fig. 12 for the current averaged over the entire pulse width (0-3 ms). The normalized relative increase (open symbols) was found by subtracting the cathode current in pure argon (zero O_2 concentration) from the current at a given oxygen partial pressure and then normalizing by the pure argon current (i.e. $[I(O_2)-I(Ar)]/ I(Ar)$). Also shown is the normalized difference (closed symbols) between the results for the two duty factors (i.e. $[RI_{10\%} - RI_{30\%}]/ RI_{10\%}$). The normalized difference is large only for small concentrations of oxygen.

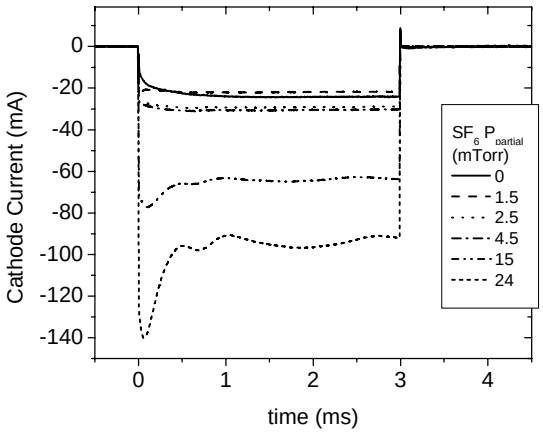

Fig. 10 Cathode current in various relative concentrations of SF_6 in argon without the applied magnetic field. Conditions were 50 mTorr total pressure, 2 kV cathode pulse, 3 ms pulse width, and a 10% duty.

The results for the current vs. applied cathode voltage measurements are summarized in Figs. 13 and 14. Fig. 13 shows the average currents over selected time spans for both pure and diluted argon (10% oxygen). The effect of oxygen is demonstrated in Fig. 14, which shows the relative difference between the results in Fig. 13 for the 0-1 ms time range and the entire pulse width. Because the voltages were slightly different for each gas mixture (< 5%), the voltage used for these results is the average value. Also shown is the difference using linear fits of the average currents over the entire pulse width. The results from Fig. 13 are not quite linear, so the relative difference from the fits vary slightly from the difference using the data. The key point, however, is that the diluents had the greatest effect at low voltage.

IV. DISCUSSION

The hollow cathode used in these experiments was open faced and as such, the electron beam is composed of secondary electrons from the cathode surface (rather than extracted plasma electrons). Nearly all secondary electrons emitted from surfaces in contact with plasmas are either photon-induced or ion-induced and, in the literature, the extent to which either contributes varies according to author. What is not disputed is the effect of surface conditions on the magnitude of the secondary electron emission coefficient (γ). In these experiments, gas adsorption will play a considerable role in altering the physical and chemical surface properties. Such changes can influence photon-induced electron emission, which requires photon energies in excess of the surface work function. Ion-induced secondary electron emission is also dependent upon the surface conditions and can be separated into two types; kinetic and potential emission. Kinetic emission results from momentum transfer to an electron, which is then energetic enough to overcome the work function. Given the large mass discrepancy between the ion and electron, kinetic emission requires a large ion velocity. Potential emission occurs when an ion, in close proximity to the surface, is neutralized by an electron tunneling from the surface conduction band. The energy released by this is sufficient to allow a second electron to enter into the gas phase. Typically this occurs when the ionization potential is more than twice the work function and has no dependence on ion velocity. Although, the probability for potential emission is small compared to kinetic emission when incident ion energies enter the keV range.

A surface in contact with a plasma is a very dynamic, with deposition countered by emission of both charged and neutral species. This is particularly true when the plasma is

modulated. In the absence of the plasma, deposition from the gas phase serves to build up an adsorbed layer. Consider for example, 1 mTorr of oxygen at room temperature. The gas density $n_g = 3.5x10^{13}$ cm^{-3} and velocity $v = 4.8x10^4$ cm/s produces a flux $F= 1.7x10^{18}$ $cm^{-2}s^{-1}$. It takes about 1 ms to accumulate one monolayer using a sticking coefficient of 1% [5]. For a plasma generated under the same conditions having a density on the order of 10^{11} cm^{-3} and an electron temperature of 0.5 eV, the ion flux would be on the order of 10^{16} cm^{-2} s. If the sticking coefficient is 1% and the sputter yield is one, the deposition rate would be balanced by the removal rate and the surface would remain gas free. It is important to recognize the importance of sticking coefficients and sputter yields in this example. In fact, these values are dependent upon the surface conditions. For example, with increasing coverage, the sticking coefficient decreases while the sputter yield will generally increase. For modulated plasma production, where periods of only deposition are followed by periods of both deposition and sputtering, a more complicated approach is required.

It is with these ideas in mind, that we discuss the results for these experiments and outline an argument for the observed results.

A. Cathode current measurement

The measured cathode current consists of both positive ions (I_i) impacting the cathode surface and negative species leaving the surface, with the dominant negative species expected to be secondary electrons (I_e). The current can be written as:

$$I_c = I_e + I_i = \gamma I_i + I_i = I_i(1+\gamma), \tag{3}$$

where γ is the secondary emission coefficient. An increase or decrease in measured cathode current will thus reflect an increase or decrease in ion current and/or secondary electron emission. Most likely it reflects an increase in both, since an increase in secondary electrons will increase ionization in the hollow cathode, resulting in a larger ion current. It is worth noting that the equation ignores photon, fast neutral, or metastable-induced secondary emission. However for most conditions in this work, ion-induced secondary emission is expected to be the dominant source of electrons [6].

The cathode in this work is brass, a copper-zinc alloy, and the secondary electron yields for clean brass are unknown. However, the yields for copper were found to be in the range of 0.2 to 0.8 for 2.0 keV Ar^+ ions [6,7,8], while the yields for zinc are about 75% those of copper [8]. Generally, ions with a lower mass would have a greater yield than heavier ions [8]. This was observed for molecular nitrogen and oxygen compared to argon ions impacting single crystal <100> tungsten in the kilovolt range [9], although this mass relationship should not be extrapolated to all molecular ions and all substrates. In the case of substrates with some form of adsorbate on the surface (for which the brass data exists), the yields are approximately an order of magnitude higher than clean substrates upon 2 keV Ar^+ ion impact [6]. Given this large difference, it becomes important to consider cathode currents for various operating conditions, particularly background gas.

B. Gas comparison

The results of Fig. 11 show an increase in cathode current with increasing oxygen and SF_6 concentrations. Increasing nitrogen concentrations, on the other hand, show a decrease in current.

It is difficult to explain these results using only gas-phase relationships. The total ionization cross-sections for nitrogen and oxygen are virtually identical and are a maximum of 25% higher than that of argon from 0.2 to 2.0 keV [10]. For SF_6, the cross section is nearly 4 times greater than argon over a similar range of energies [11]. The addition of molecular species, however, will provide an additional charge destruction mechanism when compared to argon in the form of electron-ion recombination. The rates are significant and should offset any increase in production rates, thereby lowering the steady-state plasma density and in turn, reducing the cathode current. This reduction is only observed for nitrogen.

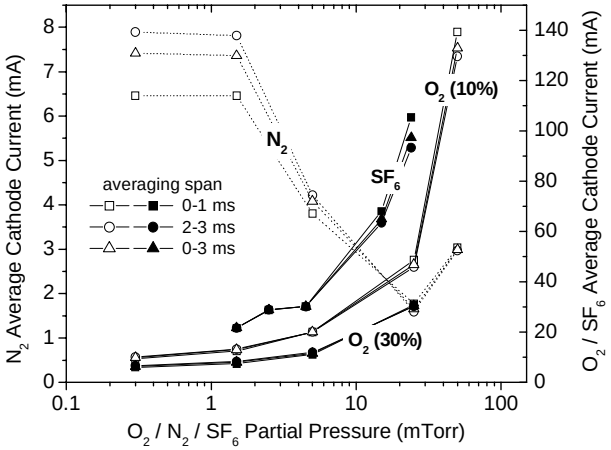

Fig. 11 Summary of non-magnetized cathode operation as a function of O_2, N_2, and SF_6 partial pressure. The currents were averaged over different fractions of the pulse time, as indicated.

However, it is well known that adsorbed gas on a surface will influence the secondary emission coefficient and depending on the adsorbate, metal, and projectile characteristics, will either increase or decrease the electron yield [12]. It is important to consider the adsorption of these gases at the surface of the cathode. The adsorption on brass is unknown but for copper, N_2 at room temperature will not form a strong bond and resides on the surface as a molecule [13]. This would suggest the adsorption is limited to a monolayer and exclude the formation of any nitride (Atomic nitrogen however, strongly reacts with copper surfaces.). Oxygen on the other hand, will form a strong bond and dissociatively chemisorbs as atoms on the surface [13], thereby increasing the likelihood of oxide formation. It is also worth noting that the work function of both copper and zinc are lower than the surface work function when oxygen is adsorbed [14]. The behavior of SF_6 is unknown but given that it's electronegative like O_2 (much stronger so), it is assumed to dissociate and strongly bond to copper as either sulfur or fluorine.

The above discussion applies mainly when the plasma is off. When the plasma is on, the surface should evolve in quite a different manner. Nitrogen atoms will react with copper (and presumably brass), and it is expected that the nitride formation would occur in the presence of the plasma. Ion beam studies of N_2^+ and N^+ ions impacting Cu(100) with energies from 20 to 800 eV, have shown the presence of both surface and subsurface nitrogen [15]. Surface species likely result from a flux of atomic ions and the dissociation of molecular ions when they strike the surface. The subsurface species are probably the result of ion implantation at higher energies (> 200 eV). In glow discharge sputtering of brass cathodes in nitrogen plasmas [16], the incorporation of nitrogen was found to extend as deep as 6 nm with a peak relative atomic concentration of N of approximately 0.75 at roughly 3 nm. For these results, the discharge was operated for about 24 hours, the pressure was 110

mTorr, the discharge current was 0.5 mA/cm^2, and the ion energy was estimated to be 700 eV. It is also worth noting that Cu is preferentially sputtered over Zn, and at the peak nitrogen concentration the concentrations are 0.15 and 0.1 respectively, compared to the bulk values of 0.63 and 0.37.

The formation of an oxide or nitride layer on the surface is an important consideration since there is evidence that such layers at the surface can increase the secondary electron emission. For oxidized metal surfaces, emission is almost always larger [17]. Similar data for metal nitrides is more difficult to find. However, in reactive sputter deposition, a decrease in the target voltage (at constant power operation) is an indication of increasing secondary electron emission and typically, when the partial pressures of both oxygen and nitrogen reaches some critical value, the target voltage decreases [18]. For reactive sputter deposition of copper nitride [19], this was found to be true. On the other hand, small oxygen, nitrogen, or other gas coverage (up to a monolayer) can result in a decrease in the yields [20,21].

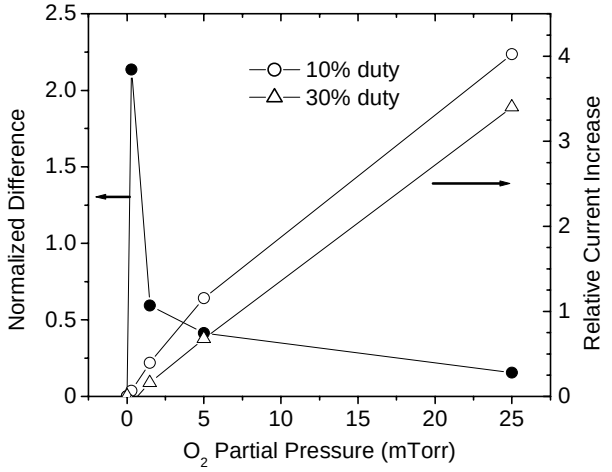

Fig. 12 Change in cathode current as a function of O_2 partial pressure. Open symbols show the relative increase with respect to pure argon (zero O_2) at 10% and 30% duty. The solid symbols represent the normalized difference between the results for 10% and 30% duty.

While the available support in the literature remains incomplete, it could be inferred that the discharge current increases with the addition of oxygen and SF_6 because of a larger secondary emission coefficients resulting from adsorbed gas on the surface. In the case of oxygen, the formation of metal-oxide layers is likely, given the interaction of oxygen with the brass (Cu and Zn) cathode both while the plasma is on and off. A similar explanation could be expected for SF_6 because of the similarities in reactivity. The results for nitrogen remain difficult to understand. If, however, nitrogen adsorption is limited to a thin molecular layer and the plasma duration is short enough such that nitrogen incorporation leading to metal-nitride formation is limited [22], it is plausible that there is no significant change in the secondary emission coefficient. In that case, gas-phase reactions lead to a reduction in the plasma density and cathode current.

C. Duty factor comparison

If adsorbed gas does increase the secondary emission coefficient, one would expect an increase in emission with increasing adsorption. To further explore this, the cathode was operated in oxygen at different duty factors and Fig. 11 shows a lower cathode current when the cathode is operated at higher duty factors. A more careful analysis using normalized current differences as a function of oxygen concentration (see Fig. 12), indicates that not only

is the cathode current larger at lower duty factors, but the difference is greatest at lower oxygen concentrations. To better understand these results, consider the following: The amount of time off in the case of 10% duty is roughly 27 ms, while at 30% it is 7 ms. A longer exposure to oxygen, in the absence of plasma, would thus allow for a thicker adsorbed layer. This is only true for a *constant* sticking coefficient. It is known, however, that the sticking coefficient decreases with coverage [23] and so for large oxygen concentrations, the coverage saturation would be largely independent of off time (or duty factor). This effect could explain the larger current seen at lower duty factors and the larger relative difference seen between high and low duty factor operation at low oxygen partial pressures.

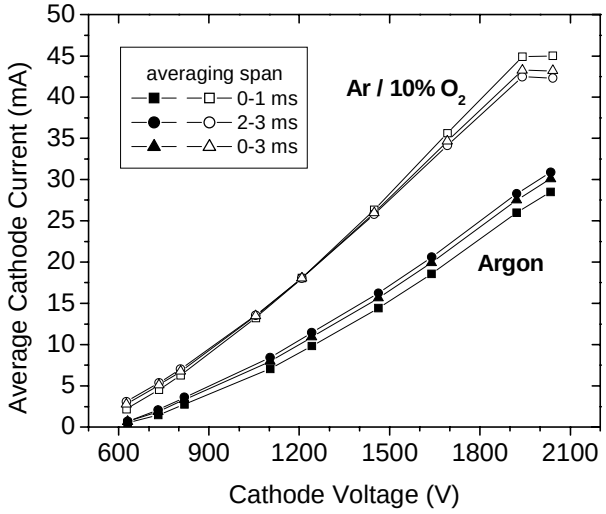

Fig. 13 Summary of the results shown in Fig. 8 for cathode currents averaged over different fractions of the pulse time, as indicated.

D. Cathode current vs. applied voltage

The results of Figs. 13 and 14 are interesting for a number of reasons. First, the trends in current vs. voltage for both pure argon and Ar/(10%)O_2 indicate a nearly linear relationship for energies above 1.2 keV (slightly higher in pure argon), before leveling off at low energies. This type of behavior is similar to ion-induced secondary electron yield measurements over energies commensurate with the applied cathode bias [24]. For yield measurements, it is argued that the emission mechanism at low energies will have a contribution from potential effects, which only requires that the incoming ion's ionization potential (E_{ip}) is at least twice the target work function (φ) and thus has no kinetic energy threshold. The yield can be expressed quantitatively as [25],

$$\gamma_{pe} = \alpha(\beta E_{ip} - 2\varphi). \tag{4}$$

At higher energies the yield varies linearly with kinetic energy [12].

Another interesting observation is the relative difference between currents at low voltages. While it was previously argued that the yields for oxides exceeds that for clean metals, one must also note that the data for 10% O_2 mixtures will contain some amount of O_2^+ and to a lesser extent, O^+ ions. From the potential emission relationship above, one might expect a smaller difference at low energies, given the lower ionization potential of O_2^+ (12.3

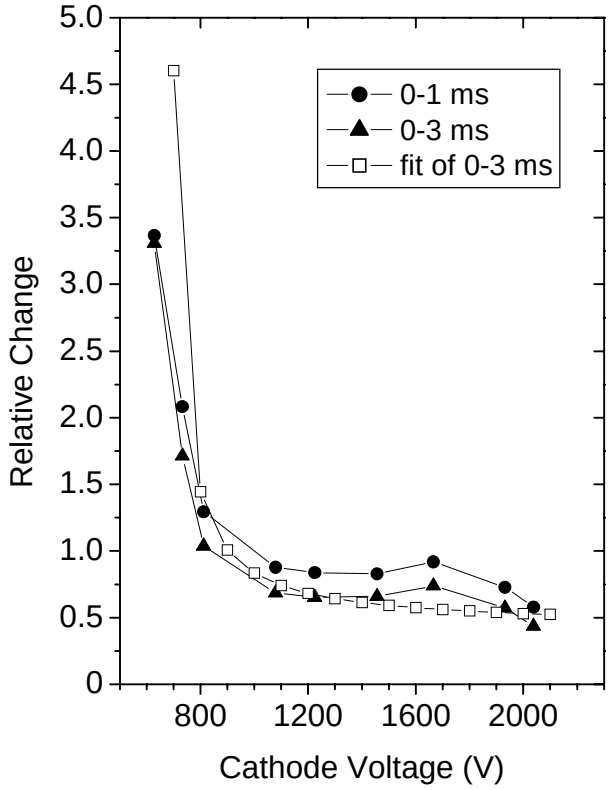

Fig. 14 Relative difference between the pure argon and 10% O_2 dilution results of Fig. 8. Solid symbols represent the difference between data points and the open squares are the difference between best fits of the 0-3 ms average data.

eV) compared to Ar^+ ions (15.7 eV). However, the lower average mass of the oxygen ions compared to argon could lead to a larger kinetic emission and would indicate potential emission is not as important for the oxygen covered surface. Indeed, the linear relationship for the Ar/(10%)O_2 extends to lower applied cathode voltages and the relative difference is more constant for cathode voltages above 1 kV.

The trends in Figs. 13 and 14 could suggest ion-induced secondary electron emission is the dominant source of electrons for sustaining the plasma over the cathode voltages in this work. However, this completely disregards well-known discharge physics, which predicts an increase in discharge current with voltage when in the abnormal glow regime, independent of emission. That is not to say the observed increase in cathode current must depend on only one effect. Indeed, it is likely a combination of both surface and discharge phenomenon.

E. Time-dependent secondary electron yield

The above data clearly shows the influence of operating atmosphere on the cathode current, and the above arguments suggest the main reason for the observed increase in oxygen and SF_6 backgrounds is an increase in the ion-induced secondary electron yield, which is caused by adsorbed gas. In order to understand this behavior, consider the relationship of Eq. 1.3 and assume the increase in cathode current with increasing oxygen concentration is simply due to an increase in the secondary emission coefficient. In this approximation, the increase in cathode current at a given concentration of oxygen is the product of the pure argon current and the emission coefficient. Its evident however that this relationship is not valid early in time, and so in order to explain the results using only secondary emission, a time-dependent secondary electron yield must be considered. By

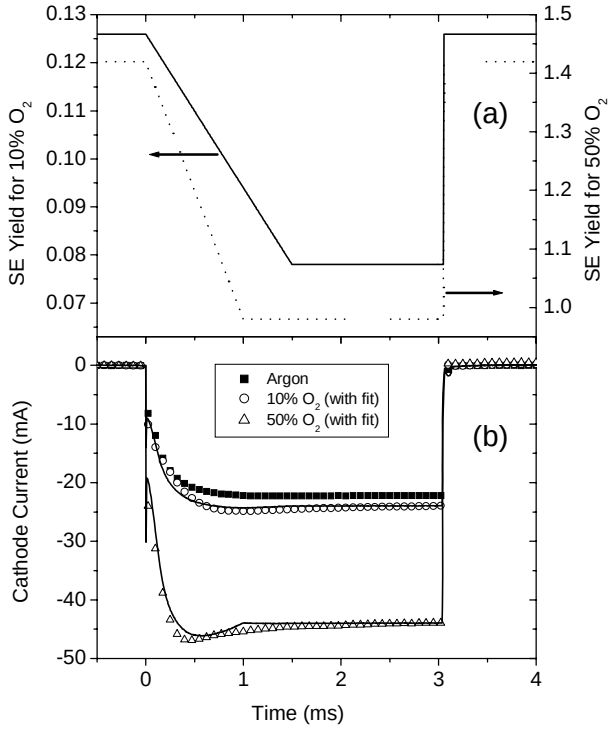

Fig. 15 Model of a time-dependent secondary electron emission coefficient. (a) Time-dependent emission coefficients for 10% and 50% O_2 dilutions and (b) the resulting calculated cathode currents using those coefficients along with the measured cathode currents.

inspection, the variation in the coefficient must occur early in time in order to achieve the results observed for larger concentrations of molecular gas (> 10%). Using the relationship of Eq. 3, a time-dependent emission coefficient was determined by a best-fit approach using the measured currents; the results are shown in Fig. 15. Time-dependent emission coefficients are shown in Fig. 15 (a), and the calculated cathode currents using those coefficients are shown by lines in Fig. 15(b), along with the measured currents indicated by symbols.

While these simple models are clearly inadequate, given that no plasma physics or gas-phase chemistries are considered, the results are useful in illustrating how the emission of electrons influences cathode operation. The physical basis for a time-dependent emission coefficient is not unreasonable, given the relationship to adsorbate coverage and the dynamic nature of the cathode surface in pulsed plasma generation. The temporal behavior of the secondary emission coefficient shown in Fig. 15 would be similar to the cathode surface coverage in that it would be highest right before plasma ignition, a period of only gas adsorption. The coefficient would then decrease due the weakly bound gas species (physisorption) are removed by ion impact. Finally, the coefficient would reach some steady state value once the removal is balanced by adsorption. It is important to recognize that the complete removal of gases from the surface is very unlikely in this work since the neutral-ion flux ratio is ~ 100, for 1 mTorr and a 10^{11} cm^{-3} plasma density.

It is also interesting to note that for the case of 10% oxygen background, the emission coefficients are not far from a commonly accepted yield of 10%. In the case of 50% oxygen concentration, yields above 100% are required but, as noted above the yields for oxide coatings can be quite high.

V. SUMMARY AND CONCLUSION

The Naval Research Laboratory's Large Area Plasma Processing System (LAPPS) uses hollow cathode discharges to generate the high-energy electron beams that form the plasma source in the processing system. In these experiments, pulsed hollow cathode operation was investigated in a variety of pure and diluted background gases. Particular attention was focused on argon diluted with nitrogen, oxygen, and SF_6. Generally, for varied operating conditions (applied voltage, duty factor) the cathode current was found to increase with increasing concentrations of both oxygen and SF_6, but for nitrogen, the current was found to *decrease* with increasing nitrogen concentrations. The results were explained by considering the adsorption of gases on the surface of the cathode, which can cause an increase in the ion-induced secondary electron emission. During the pulse, temporal dependencies in the cathode current were evident and depended on the relative concentration of the molecular gases. These behaviors were considered in the context of a simple time-dependent secondary emission coefficient, which, in the absence of a more comprehensive plasma model, could capture the general observed behavior.

The results are interesting but limited. A more careful study is required to fully understand the influence of background gas on pulsed, hollow cathode operation. One complicating aspect of this work is the use of brass cathodes since there is not much supporting work available in the literature. Indeed, much of the adsorption discussion is based on the brass constituents, rather than the brass. Other LAPPS cathodes are constructed from stainless steel and while more common, there is again limited supporting evidence in the literature. A more definitive study would involve cathode material that is well understood in terms of gas adsorption. Aluminum is a good choice given that it is non-magnetic and has well-known adsorption properties.

VI. ACKNOWLEDGMENT

This work was supported by the Office of Naval Research.

APPENDIX A

For the ion flux in oxygen mixtures shown in Fig 2a, it is apparent that gas phase reactions alone cannot fall short of explaining the measured temporal behavior. The total ion flux peaks at about 215 μs after the plasma initiation (the small offset from t = 0 is due to the time-of-flight in the mass spectrometer) and has a FWHM of approximately 340 μs. The characteristic decay times (1/e) taken from the peak in the flux measurements are $\tau(O_2^+)$ = 158 μs, $\tau(Ar^+)$ = 175 μs, and $\tau\ (O^+)$ = 165 μs. Gas phase electron-ion and ion-ion reactions are important destruction mechanisms in these plasmas [26]:

$O_2^+ + e^- \rightarrow 2O$; $\quad k_a = 2x10^{-8}\ T_e^{-1/2}\ cm^3/s$

$O^+ + O_2 \rightarrow O + O_2^+$; $\quad k_a = 2x10^{-11}\ cm^3/s$

$Ar^+ + O_2 \rightarrow Ar + O_2^+$; $\quad k_a = 5x10^{-11}\ cm^3/s$

Assuming a plasma density of $1x10^{11}\ cm^{-3}$, T_e = 0.5 eV, and 25 mTorr O_2, we find $\tau(O_2^+)$ = 350 μs, $\tau(Ar^+)$ = 22 μs, and $\tau\ (O^+)$ = 55 μs. Clearly, these gas phase reactions cannot account for the temporal behavior of the ion flux. Most importantly can't account for the peak in the ion fluxes.

APPENDIX B

The model used for the time-dependent emission coefficient and resulting current was done in an "Origin" spreadsheet using a code developed with "Lab Talk". The emission coefficient (Fig. 15(a)), was found by assuming a constant yield value before (and after) the high voltage pulse, a linearly decreasing value during a fraction of the pulse, and a constant value for the remainder of the pulse. The cathode currents in the gas mixtures were then calculated using Eq. 3, where I_i is the cathode current in the pure argon and I_c is the cathode currents in the gas mixtures. The spreadsheet script was:

```
sta=1.42        (starting secondary emission yield coefficient)
fin=0.980       (steady-state secondary emission yield)
de=(sta-fin)/200        (data points to get to steady-state; time)
loop (ii,1,100){col(se)[ii]=sta}        (pre-pulse yield)
loop (ii,101,301){col(se)[ii]=sta-((ii-101)*de)}        (linear drop in yield)
loop (ii,302,711){col(se)[ii]=col(SE)[301]}  (steady-state yield)
loop (ii,712,1002){col(se)[ii]=sta}     (post-pulse yield)
col(IcSE)=col(Ica)+(col(se)*col(Ica))          ( IcSE = cathode current in mixture;
                                                 Ica = cathode current in pure Argon)
```

REFERENCES

[1] J.J. Rocca, J.D. Meyer, M.R. Farrell, and G.J. Collins, J. Appl. Phys. **56**, 790 (1984).

[2] Both types of electron guns are available, although development of a "closed face" sheet electron beam gun was halted due to unsuitable beam characteristics. Recently, development was resumed.

[3] S.G. Walton and D. Leonhardt in 48th Annual Society of Vacuum Coaters Technical Conference Proceedings, 5 (2005).

[4] Scott G. Walton, Darrin Leonhardt, and Richard F. Fernsler, IEEE Trans. Plasma Sci. **33 (2)**, 838 (2005).

[5] One monolayer is defined as 1.7×10^{15} cm^{-2} and is produced by an exposure of one Langmuir (L) at room temperature assuming a sticking coefficient of one: 1 L = 10^{-6} Torr s = 3.55×10^{10} cm^{-3} s.

[6] AV Phelps and Z Lj Petrovic, Plasma Sources Sci. Technol. **8**, R21(1999).

[7] B. Szapiro and J.J. Rocca, J. Appl. Phys. **65**(9), 3713 (1989).

[8] P.C. Zalm and L.J. Beckers, Surf. Sci. **152/153**, 135 (1985).

[9] N Cook and R.B. Burtt, J. Phys. D **8**, 800 (1975).

[10] H. C. Straub, P. Renault, B. G. Lindsay, K. A. Smith, and R. F. Stebbings, Phys. Rev. A **52**, 1115-1124 (1995); Phys. Rev. A **54**, 2146-2153 (1996).

[11] L.G. Christophorou and J.K. Olthoff, J. Phys. Chem. Ref. Data **29**, 267 (2000).

[12] R.A. Baragiola, in Low Energy Ion-Surface Interactions, edited by J. Wayne Rabalis (John Wiley and Sons, New York, 1994), Ch. 4.

[13] M.A. van Daelen, M. Neurock, and R.A. van Santen, Surface Science **417**, 247 (1998).

[14] Mohamed Akbi and Andre Lefort, J. Phys. D **31**, 1301 (1998).

[15] H. Yu and K.T. Leung, J. Vac. Sci. Technol A **16**, 30 (1998).

[16] Z. Wronski and J. Sielanko, Vacuum **78**, 605 (2005).

[17] D. Hasselkamp, in Particle Induced Electron Emission II, edited by G. Hohler (Springer-Verlag, New York, 1992), pp 68.

[18] W.D. Sproul, D.J. Christie, D.C. Carter, Thin Solid Films **491**, 1 (2005).

[19] D. Depla, J. Haemers, R. De Gryse, Plasma Source. Sci. Technol. **11**, 91 (2002).

[20] Unknown adsorbate but it was likely some type of oxygen coverage resulting from primarily water on Mo; Ion energies up to ~ 2 keV; P. Mahadevan, G.D. Magnuson, J.K. Layton, and C.E. Carlston, Phys. Rev. **140**, 1407 (1965).

[21] N_2 adsorption on W; Ar^+ energies up to 1 keV; Homer D. Hagstrum, Phys. Rev. **104**, 1516 (1956).

[22] One interesting observation is the increase in cathode current between 50% and 100% nitrogen concentration. It is feasible that a threshold in either nitrogen concentration or perhaps duty factor exists for metal-nitride formation.

[23] P.A. Redhead, J.P. Hobson, E.V. Kornelsen, The Physical Basis of Ultrahigh Vacuum (American Institute of Physics, New York, 1993), p. 66.

[24] P. Mahadevan, G.D. Magnuson, J.K. Layton, amd C.E. Carlston, Phys. Rev. **140**, 1407 (1965); Y. Yamauchi and R. Shimizu, Jap. J. of Apll. Phys. **22**, L227 (1983).
[25] P. Varga and H. Winter in Particle Induced Electron Emission II, edited by G. Hohler (Springer-Verlag, New York, 1992), pp 68
[26] Y. Ikezoe, S. Matsuoka, M. Takebe, and A. Viggiano, Gas Phase Ion-Molecule Reaction Rates Through 1986 (published by the Ion Reaction Research Group of The Mass Spectroscopy Society of Japan; Distributed by Maruzen Co., Ltd., Tokyo, Japan, 1989).